

# Revisiting the hypertriton lifetime puzzle

A. Pérez-Obiol,<sup>1</sup> D. Gazda,<sup>2</sup> E. Friedman,<sup>3</sup> and A. Gal<sup>3,\*</sup>

<sup>1</sup>Laboratory of Physics, Kochi University of Technology, Kami, Kochi 782-8502, Japan

<sup>2</sup>Nuclear Physics Institute, 25068 Řež, Czech Republic

<sup>3</sup>Racah Institute of Physics, The Hebrew University, Jerusalem 91904, Israel

(Dated: July 9, 2020)

Conflicting values of the hypertriton ( ${}^3_\Lambda\text{H}$ ) lifetime were extracted in recent relativistic heavy-ion collision experiments. The ALICE Collaboration's reported  ${}^3_\Lambda\text{H}$  lifetime  $\tau({}^3_\Lambda\text{H})$  is compatible within measurement uncertainties with the free  $\Lambda$  lifetime  $\tau_\Lambda$ , as naively expected for a loosely bound  $\Lambda$  hyperon in  ${}^3_\Lambda\text{H}$ , whereas the STAR Collaboration's reported range of  $\tau({}^3_\Lambda\text{H})$  values is considerably shorter:  $\tau_{\text{STAR}}({}^3_\Lambda\text{H}) \sim (0.4-0.7)\tau_\Lambda$ . This  ${}^3_\Lambda\text{H}$  lifetime puzzle is revisited theoretically, using  ${}^3_\Lambda\text{H}$  three-body wavefunctions generated in a chiral effective field theory approach to calculate the decay rate  $\Gamma({}^3_\Lambda\text{H} \rightarrow {}^3\text{He} + \pi^-)$ . Significant but opposing contributions arise from  $\Sigma NN$  admixtures in  ${}^3_\Lambda\text{H}$  and from  $\pi^-$ - ${}^3\text{He}$  distorted waves. Evaluating the inclusive  $\pi^-$  decay rate  $\Gamma_{\pi^-}({}^3_\Lambda\text{H})$  via a branching ratio  $\Gamma({}^3_\Lambda\text{H} \rightarrow {}^3\text{He} + \pi^-)/\Gamma_{\pi^-}({}^3_\Lambda\text{H})$  determined in helium bubble-chamber experiments, and adding  $\Gamma_{\pi^0}({}^3_\Lambda\text{H})$  through the  $\Delta I = \frac{1}{2}$  rule, we derive  $\tau({}^3_\Lambda\text{H})$  assuming several different values of the  $\Lambda$  separation energy  $B_\Lambda({}^3_\Lambda\text{H})$ . It is concluded that each of ALICE and STAR reported  $\tau({}^3_\Lambda\text{H})$  intervals implies its own constraint on  $B_\Lambda({}^3_\Lambda\text{H})$ :  $B_\Lambda \lesssim 0.1$  MeV for ALICE,  $B_\Lambda \gtrsim 0.2$  MeV for STAR.

PACS numbers:

**Introduction.** The hypertriton,  ${}^3_\Lambda\text{H}$ , a  $\Lambda pn$  bound state with isospin  $I=0$  and spin-parity  $J^P = \frac{1}{2}^+$ , is the lightest bound  $\Lambda$  hypernucleus [1]. Given the tiny  $\Lambda$  separation energy  $B_\Lambda({}^3_\Lambda\text{H}) = 0.13 \pm 0.05$  MeV [2], implying a  $\Lambda$ -deuteron mean distance of about 10 fm, the  ${}^3_\Lambda\text{H}$  decay rate is expected to be close to that of the free  $\Lambda$  hyperon which to 99.7% is governed by the nonleptonic  $\Lambda \rightarrow N\pi$  weak-decay mode. This expectation was quantified using a  $3N$  final-state closure approximation in early  ${}^3_\Lambda\text{H}$  lifetime calculations [3] leading to an estimate  $\Gamma({}^3_\Lambda\text{H})/\Gamma_\Lambda = 1 + 0.14\sqrt{B_\Lambda}$  ( $B_\Lambda$  in MeV), thereby suggesting a roughly 5% enhanced  ${}^3_\Lambda\text{H}$  decay rate  $\Gamma({}^3_\Lambda\text{H})$  with respect to the free  $\Lambda$  decay rate  $\Gamma_\Lambda$ , i.e.  $\tau({}^3_\Lambda\text{H}) \approx 0.95\tau_\Lambda$ . Yet values of  $\tau({}^3_\Lambda\text{H})$  considerably shorter than  $\tau_\Lambda$  were reported recently by two of the three relativistic heavy ion (RHI) experiments (HypHI and STAR) listed in Table I, in distinction from ALICE most recent value which within its own uncertainties agrees with  $\tau_\Lambda$ . In fact, a similarly large spread of  $\tau({}^3_\Lambda\text{H})$  values, and with bigger uncertainties, had been reported in old nuclear emulsion and helium bubble-chamber (BC) hypernuclear measurements [5]. Finally, as if to compound confusion, STAR just published a  $B_\Lambda({}^3_\Lambda\text{H})$  range of values [13] higher than listed above and completely outside the range of values considered in modern  ${}^3_\Lambda\text{H}$  lifetime calculations. Implications to heavier hypernuclei are discussed in Ref. [14].

Table I also lists the only two three-body calculations of  $\tau({}^3_\Lambda\text{H})$  published since 1998. Kamada *et al.* [11] reached a value shorter by merely a few percent than  $\tau_\Lambda$  within a complete Faddeev calculation, dealing with *all* three  $\pi^-$  final-state channels:  ${}^3\text{He} \pi^-$ ,  $dp\pi^-$  and  $ppn\pi^-$ , while using the  $\Delta I = \frac{1}{2}$  rule to add the  $\pi^0$  decay channels. However, the SC89 hyperon-nucleon ( $YN$ ) Nijmegen interaction [15] used there to construct a three-body  ${}^3_\Lambda\text{H}$

TABLE I:  ${}^3_\Lambda\text{H}$  lifetime values  $\tau({}^3_\Lambda\text{H})$  and  $\pi^-$  branching ratios  $R_3 = \Gamma({}^3_\Lambda\text{H} \rightarrow {}^3\text{He} + \pi^-)/\Gamma_{\pi^-}({}^3_\Lambda\text{H})$  extracted in recent RHI experiments, and from two three-body calculations. Note:  $\tau_\Lambda = 263 \pm 2$  ps [4],  $R_3(\text{BC world average}) = 0.35 \pm 0.04$  [5].

	Collaboration	$\tau({}^3_\Lambda\text{H})$ in ps	$R_3$
Exp	HypHI [6]	$183^{+42}_{-32} \pm 37$ [6]	–
Exp	STAR [7, 8]	$142^{+24}_{-21} \pm 29$ [8]	$0.32 \pm 0.05 \pm 0.08$
Exp	ALICE [9, 10]	$242^{+34}_{-38} \pm 17$ [10]	–
Th	Kamada <i>et al.</i> [11]	256	0.379
Th	Gal-Garcilazo [12]	$213 \pm 5$	0.357

wavefunction does poorly in hypernuclei, beginning with  $A=4$  [16]. The other calculation [12] derived  $\tau({}^3_\Lambda\text{H})$  shorter than  $\tau_\Lambda$  by  $\sim 20\%$ , half of which arising from attractive final-state interaction (FSI) of the outgoing pion. We comment below on each of these works.

In this Letter we report a new evaluation of the decay rate  $\Gamma({}^3_\Lambda\text{H} \rightarrow {}^3\text{He} + \pi^-)$  using  ${}^3_\Lambda\text{H}$  wavefunctions generated in chiral effective field theory ( $\chi\text{EFT}$ ) leading-order (LO)  $YN$  interaction model [17, 18] that was used successfully in *ab initio* calculations of  $A=3,4$  hypernuclear binding energies [19–21]. Surprisingly, the  $\lesssim 0.5\%$  norm  $\Sigma NN$  admixtures reduce by  $\approx 10\%$  the purely  $\Lambda NN$  decay rate. In contrast, using realistic low-energy  $\pi^-$ - ${}^3\text{He}$  distorted waves (DW) rather than plane waves (PW) enhances  $\Gamma({}^3_\Lambda\text{H} \rightarrow {}^3\text{He} + \pi^-)$  by  $\approx 15\%$ . Other  $\pi^-$  partial decay rates are included by using the BC branching ratio value  $R_3 = \Gamma({}^3_\Lambda\text{H} \rightarrow {}^3\text{He} + \pi^-)/\Gamma_{\pi^-}({}^3_\Lambda\text{H}) = 0.35 \pm 0.04$  [5] which agrees with  $R_3$  values listed in Table I. Adding the inclusive  $\pi^0$  decay rate,  $\Gamma_{\pi^0}({}^3_\Lambda\text{H}) = \Gamma_{\pi^-}({}^3_\Lambda\text{H})/2$  by the  $\Delta I = \frac{1}{2}$  rule, we provide a new theoretical statement about  $\tau({}^3_\Lambda\text{H})$  and its relationship to  $B_\Lambda({}^3_\Lambda\text{H})$  for each of the three RHI experiments listed in Table I.

**Form factors.** To relate  $\Gamma(\Lambda^3\text{H} \rightarrow \Lambda^3\text{He} + \pi^-)$  to the free- $\Lambda$  partial decay rate  $\Gamma(\Lambda \rightarrow p\pi^-)$  we follow Kamada *et al.* [11], Eq. (A5), writing down  $\Gamma(\Lambda \rightarrow p\pi^-)$  in the form

$$\frac{\Gamma_{\Lambda \rightarrow p\pi^-}}{(G_F m_\pi^2)^2} = \frac{k_{\pi^-}}{\pi} \frac{M_p}{M_p + \omega_{\pi^-}} \left[ \mathcal{A}_\Lambda^2 + \mathcal{B}_\Lambda^2 \left( \frac{k_{\pi^-}}{2\bar{M}} \right)^2 \right], \quad (1)$$

with  $k_{\pi^-}=100.6$ ,  $\omega_{\pi^-}=172.0$ ,  $\bar{M}=\frac{1}{2}(M_p+M_\Lambda)=1027$ , all in MeV,  $G_F m_\pi^2=2.21 \cdot 10^{-7}$  and where  $\mathcal{A}_\Lambda=1.024$ ,  $\mathcal{B}_\Lambda=-9.431$  are chosen here to satisfy the new value [4] of the  $\Lambda \rightarrow p\pi^-$  asymmetry parameter [22]. With these values one obtains  $\Gamma(\Lambda \rightarrow p\pi^-)=2.534$  GHz, and adding half of it for  $\Gamma(\Lambda \rightarrow n\pi^0)$  to respect the  $\Delta I=\frac{1}{2}$  rule leads to  $\tau_\Lambda \approx \tau(\Lambda \rightarrow N\pi)=\Gamma^{-1}(\Lambda \rightarrow N\pi)=263.1$  ps. The squares of  $\mathcal{A}_\Lambda$  and  $\mathcal{B}_\Lambda$  above arise from a  $\Lambda \rightarrow p\pi^-$  parity violating (PV) spin-independent amplitude  $\mathcal{A}_\Lambda$  and a parity conserving (PC) spin-dependent amplitude  $\mathcal{B}_\Lambda \vec{\sigma} \cdot \hat{k}_{\pi^-}$ , respectively. The PV contribution in Eq. (1) dominates with 83% of  $\Gamma(\Lambda \rightarrow p\pi^-)$ .

Proceeding to  $\Gamma(\Lambda^3\text{H} \rightarrow \Lambda^3\text{He} + \pi^-)$ , we introduce two nuclear form factors that accompany the  $\Lambda \rightarrow p\pi^-$  amplitudes:  $\mathcal{A}_\Lambda \rightarrow \mathcal{A}_\Lambda F^{\text{PV}}(\vec{q})$  and  $\mathcal{B}_\Lambda \vec{\sigma} \cdot \hat{k}_{\pi^-} \rightarrow \mathcal{B}_\Lambda F^{\text{PC}}(\vec{q})$ . These form factors are defined by

$$F^{\text{PV}}(\vec{q}) = \int \Phi_f^*(\vec{R}, \vec{r}_3) \phi_\pi(\vec{q}; \vec{r}) \Phi_i(\vec{R}, \vec{r}_3) d^3 r_3 d^3 R, \quad (2)$$

$$F^{\text{PC}}(\vec{q}) = \int \Phi_f^*(\vec{R}, \vec{r}_3) \phi_\pi(\vec{q}; \vec{r}) \vec{\sigma} \cdot \hat{q} \Phi_i(\vec{R}, \vec{r}_3) d^3 r_3 d^3 R, \quad (3)$$

where the initial  $\Lambda^3\text{H}$  and final  $\Lambda^3\text{He}$  three-body wavefunctions  $\Phi_{i,f}$  are written explicitly in terms of Jacobi coordinates:  $\vec{R}$  for the relative coordinate of spectator nucleons 1 and 2 and  $\vec{r}_3$  for the coordinate of the third, ‘active’ baryon relative to the c.m. of the spectator nucleons. The suppressed spin-isospin variables of  $\Phi_{i,f}$  are fully taken into account. In these expressions  $\phi_\pi(\vec{q}; \vec{r})$  is a DW  $\pi^-$  wavefunction evolving via FSI from a PW pion with momentum  $\vec{q}$  in the  $\Lambda^3\text{H}$  rest frame. Its argument  $\vec{r} = \frac{2}{3}\vec{r}_3$  is identified with the coordinate of the active baryon with respect to the c.m. of  $\Lambda^3\text{He}$ . Expanding  $\phi_\pi$  in partial waves  $\ell_\pi$ , and recalling the spin-parity assignment  $J^P=\frac{1}{2}^+$  for both  $\Lambda^3\text{He}$  and  $\Lambda^3\text{H}$ , it follows that the only  $\ell_\pi$  values allowed are  $\ell_\pi=0,2$ . Numerically we find a negligible  $\ell_\pi=2$  contribution to  $\Gamma(\Lambda^3\text{H} \rightarrow \Lambda^3\text{He} + \pi^-)$  of order 0.1%, proceeding exclusively through the relatively minor PC amplitude. Keeping to  $\ell_\pi=0$ , it is straightforward to show that  $F^{\text{PC}} = \frac{1}{3}F^{\text{PV}}$  for the dominant deuteron-like  ${}^3S_1 - {}^3D_1$   $NN$  plus  $s$ -wave  $\Lambda$  configuration in  $\Lambda^3\text{H}$ , thereby leading to the following expression [23]:

$$\frac{\Gamma_{\Lambda^3\text{H} \rightarrow \Lambda^3\text{He} + \pi^-}}{(G_F m_\pi^2)^2} \approx \frac{q}{\pi} \frac{M_{\Lambda^3\text{He}}}{M_{\Lambda^3\text{He}} + \omega_{\pi^-}(q)} \times \left[ \mathcal{A}_\Lambda^2 + \frac{1}{9} \mathcal{B}_\Lambda^2 \left( \frac{k_{\pi^-}}{2\bar{M}} \right)^2 \right] 3|F^{\text{PV}}(q)|^2, \quad (4)$$

where the factor 3 accounts for the three final nucleons to which the  $\Lambda$  may have turned into. In Eq. (4) the pion cm momentum (energy) is  $q=114.4$  ( $\omega_{\pi^-}=179.3$ ),  $M_{\Lambda^3\text{He}}=2809$ , using charge-averaged masses  $M_N=938.92$ ,  $m_\pi=138.04$ , all in MeV. Numerically the PC contribution to  $\Gamma(\Lambda^3\text{H} \rightarrow \Lambda^3\text{He} + \pi^-)$  through the  $|\mathcal{B}_\Lambda|^2$  term is found to be  $\lesssim 3\%$  of the calculated  $\Lambda^3\text{H}$  two-body decay rate, and the error associated with assigning it a coefficient 1/9 in Eq. (4) is of order 0.1%. Nevertheless, no prior relationship between the form factors  $F^{\text{PC}}$  and  $F^{\text{PV}}$  that would lead to this coefficient 1/9 was assumed in our actual calculation of these form factors.

New  $\Sigma$ -hyperon two-body decay channels,  $\Sigma^- \rightarrow n\pi^-$  and  $\Sigma^0 \rightarrow p\pi^-$ , become available in  $\Lambda^3\text{H} \rightarrow \Lambda^3\text{He} + \pi^-$  once  $\Sigma NN$  admixtures are considered. The corresponding  $\Sigma^-$  decay amplitudes are taken from studies of its weak decay:  $\mathcal{A}_{\Sigma^-}=-1.364$ , fitted to the lifetime value  $\tau_{\Sigma^-}=147.9 \pm 1.1$  ps [4], and a negligible  $\mathcal{B}_{\Sigma^-}$  [24]. Since the  $\Sigma^0 \rightarrow p\pi^-$  weak decay in free space is superseded by the  $\Sigma^0 \rightarrow \Lambda\gamma$  electromagnetic decay we use the chiral-Lagrangian prediction  $\mathcal{A}_{\Sigma^0}=\frac{1}{\sqrt{2}}\mathcal{A}_{\Sigma^-}$  [24] and neglect  $\mathcal{B}_{\Sigma^0}$ . Using isospin basis consistent with that used in our  $\Lambda^3\text{H}$  wavefunction construction, the form factor  $F^{\text{PV}}$  in Eq. (2) is generalized according to:

$$\begin{aligned} \mathcal{A}_\Lambda F^{\text{PV}} &\rightarrow \mathcal{A}_\Lambda F_{I=0}^{\text{PV}} + \frac{1}{3}(\sqrt{2}\mathcal{A}_{\Sigma^-} + \mathcal{A}_{\Sigma^0})F_{I=1}^{\text{PV}} \\ &= \mathcal{A}_\Lambda F_{I=0}^{\text{PV}} + \frac{1}{\sqrt{2}}\mathcal{A}_{\Sigma^-} F_{I=1}^{\text{PV}}, \end{aligned} \quad (5)$$

whereas  $\mathcal{B}_\Lambda F^{\text{PC}} \rightarrow \mathcal{B}_\Lambda F_{I=0}^{\text{PC}}$ , leaving Eq. (3) as is. The subscripts  $I=0$  and  $I=1$  indicate restricting in Eqs. (2,3) the expansion of the  $\Lambda^3\text{H}$  wavefunction  $\Phi_i$  to  $I_{NN}=0$   $\Lambda NN$  or to  $I_{NN}=1$   $\Sigma NN$  components, respectively. Since the two PV amplitudes in Eq. (5) interfere upon forming their summed absolute value squared, even as small a  $\Sigma NN$  admixture probability as  $P_\Sigma \lesssim 0.5\%$  may affect considerably the calculated  $\Lambda^3\text{H}$  two-body  $\pi^-$  decay rate which is found to be *reduced* by slightly over 10% from its value disregarding  $\mathcal{A}_{\Sigma^-}$ .

**Pion distorted waves.** The DW pion wavefunction  $\phi_\pi(\vec{q}; \vec{r})$  input to the form factors  $F^{\text{PV,PC}}(\vec{q})$ , Eqs. (2,3), was generated from a standard optical potential [25, 26]. The low-energy pion-nucleus interaction is well understood in terms of optical potentials constrained by pionic atoms data across the periodic table. Here we used optical potential parameters from large scale fits to  $\pi^-$ -atom level shifts and widths, from Ne to U [27, 28], where  $s$ - and  $p$ -wave  $\pi N$  scattering amplitude parameters associated with optical potential terms linear in the nuclear density come out close to their threshold real on-shell values. Parameters associated with optical potential terms quadratic in density are phenomenological. Applying this potential to pionic atoms of  $\Lambda^3\text{He}$  it is found to reproduce the experimental  $1S$  level shift and width [29].

To extrapolate from near-threshold to  $q=114.4$  MeV in the  $\pi^- \Lambda^3\text{He}$  c.m. system we revised the above  $\pi N$

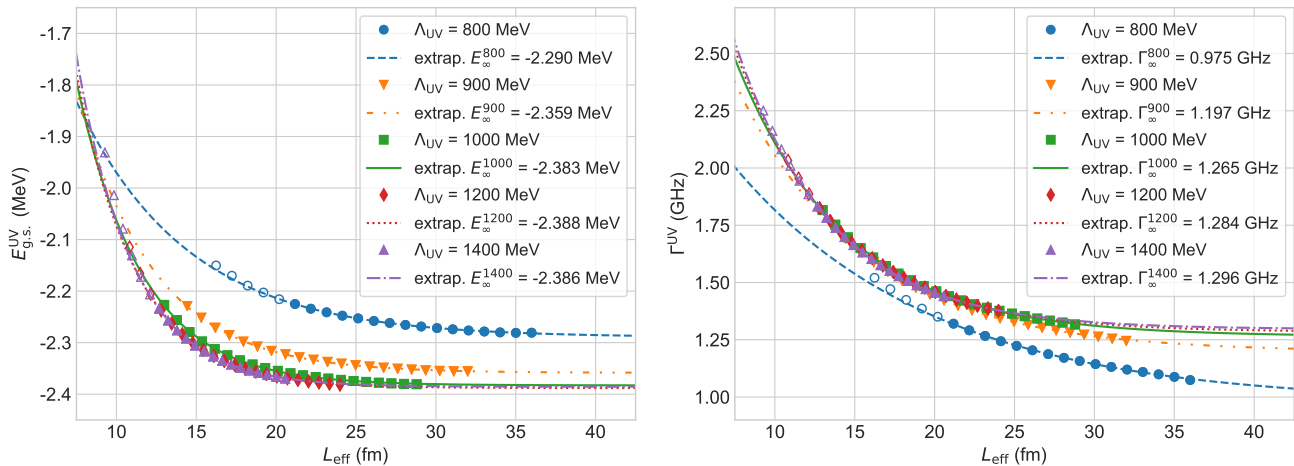


FIG. 1: (color online). Extrapolations of NCSM calculated  ${}^3_{\Lambda}\text{H}$  ground-state energies  $E_{\text{g.s.}}^{\text{UV}}(L_{\text{eff}})$  (left) and the corresponding  ${}^3_{\Lambda}\text{H} \rightarrow {}^3\text{He} + \pi^-$  decay rates  $\Gamma^{\text{UV}}(L_{\text{eff}})$  (right) as a function of the IR length  $L_{\text{eff}}$  using, e.g., Eq. (6) for several fixed UV cutoff values  $\Lambda_{\text{UV}}$ .  $N_{\text{max}}=36$  and  $\hbar\omega=14$  MeV are held fixed for  ${}^3\text{He}$ . Open symbols start at  $N_{\text{max}}=28$ . Filled symbols mark particle-stable  ${}^3_{\Lambda}\text{H}$  configurations included in the fits, starting with a variable  $N_{\text{max}}$  between 28 and 40, and up to  $N_{\text{max}}=68$ .  $\Sigma NN$  admixtures and DW pions are included in the decay-rate calculations of the right panel.

linear-density terms using scattering amplitudes from the SAID package [30]. As for the non-linear terms, we extrapolated their threshold values by using also fits to  $\pi^{\pm}$  elastic scattering at  $T_{\text{lab}}=21.5$  MeV on Si, Ca, Ni and Zr [31]. This resulted in a practically vanishing value of the  $s$ -wave term and a 65% increase of the  $p$ -wave term.

To check sensitivity of the form factors  $F^{\text{PV,PC}}(\vec{q})$ , Eqs. (2,3), to the DW pion wavefunction  $\phi_{\pi}(\vec{q}; \vec{r})$  we chose another set of optical potential parameters that fit only data of pionic atoms of  ${}^3\text{He}$  [29] and  ${}^4\text{He}$  [32]. The same parameters were then carried over to  $q=114.4$  MeV, adding the corresponding imaginary parts of the SAID scattering amplitudes [30] mentioned above. Tests made with static  $\Lambda$  and proton Hulthén wavefunctions showed that the corresponding DW form-factor integrals differed by less than 0.1%. More details will be given elsewhere.

**$YNN$  input and  $\Gamma({}^3_{\Lambda}\text{H} \rightarrow {}^3\text{He} + \pi^-)$ .** Three-body wavefunctions of  ${}^3\text{He}$  and  ${}^3_{\Lambda}\text{H}$ , input to  $F^{\text{PV}}$  and  $F^{\text{PC}}$  of Eqs. (2,3), were generated from Hamiltonians based on  $\chi\text{EFT}$  interactions: NNLOsim for  $NN + NNN$ , derived by fitting  $NN$  data up to  $T_{\text{lab}}^{\text{max}}=290$  MeV with a regulator cutoff momentum  $\Lambda_{\text{EFT}}=500$  MeV [33], and LO  $YN$  [17, 18] with  $\Lambda_{\text{EFT}}=600$  MeV. We followed the *ab initio* no-core shell model (NCSM) method within momentum-space harmonic-oscillator (HO) bases consisting of all excited states limited by  $\mathcal{E}_{\text{HO}} \leq (N_{\text{max}} + 3)\hbar\omega$  for a given HO frequency  $\omega$  [34]. The calculated  ${}^3\text{He}$  ground-state energy converges around  $N_{\text{max}}=30$  to  $E_{\text{exp}}({}^3\text{He})$ , independently of the HO frequency  $\omega$  over a wide range. In contrast, convergence for the weakly bound  ${}^3_{\Lambda}\text{H}$ , down to uncertainty of a few keV, is reached only in the largest NCSM space with  $N_{\text{max}}=70$ . Although the  ${}^3_{\Lambda}\text{H}$  energy computed at  $N_{\text{max}}=70$  exhibits a variational min-

imum for  $\hbar\omega \approx 9$  MeV, with  $B_{\Lambda}({}^3_{\Lambda}\text{H})=0.16$  MeV, the corresponding  ${}^3_{\Lambda}\text{H} \rightarrow {}^3\text{He} + \pi^-$  decay rates exhibit undesired, stronger dependence on  $\hbar\omega$ . A standard empirical solution to tame such dependence is to extrapolate  $\Gamma_{\hbar\omega}(N_{\text{max}})$ , for a fixed  $\hbar\omega$ , exponentially to  $N_{\text{max}} \rightarrow \infty$ . Here, instead, we applied a recently proposed EFT-inspired extrapolation scheme, introducing infrared (IR) length scale  $L_{\text{eff}}$  and ultraviolet (UV) momentum scale  $\Lambda_{\text{UV}}$  to the NCSM many-body HO bases [35]. Fixing  $\Lambda_{\text{UV}}$  at a sufficiently large value,  $\Lambda_{\text{UV}} \gg \Lambda_{\text{EFT}}$ , the  $\hbar\omega$  and  $N_{\text{max}}$  dependence of  $\Gamma_{\hbar\omega}(N_{\text{max}})$  may be traded off by its IR dependence on  $L_{\text{eff}}$ . Extrapolating then  $\Gamma_{\text{UV}}(L_{\text{eff}})$ , for a fixed  $\Lambda_{\text{UV}}$ , exponentially to  $L_{\text{eff}} \rightarrow \infty$ ,

$$\Gamma_{\text{UV}}(L_{\text{eff}}) = \Gamma_{\infty}^{\text{UV}} + a^{\text{UV}} \exp(-2k^{\text{UV}} L_{\text{eff}}) \quad (6)$$

with fit parameters  $a^{\text{UV}}, k^{\text{UV}}$  and  $\Gamma_{\infty}^{\text{UV}}$ , we obtained well-converged decay-rate values  $\Gamma_{\infty}^{\text{UV}}({}^3_{\Lambda}\text{H} \rightarrow {}^3\text{He} + \pi^-)$ , as shown in Fig. 1 (right panel) for several values of  $\Lambda_{\text{UV}} \geq 800$  MeV. This same procedure was applied, as shown in Fig. 1 (left panel), to extrapolate  $E_{\text{g.s.}}({}^3_{\Lambda}\text{H})=E_{\text{d}}-B_{\Lambda}$ , with  $E_{\text{d}}$  the calculated free deuteron energy. The figure exhibits UV convergence for  $\Lambda_{\text{UV}} \geq 1$  GeV, with rates  $\Gamma_{\infty}^{\text{UV}}({}^3_{\Lambda}\text{H} \rightarrow {}^3\text{He} + \pi^-)=1.28 \pm 0.02$  GHz for  $B_{\Lambda}^{\text{UV}}({}^3_{\Lambda}\text{H})=0.162 \pm 0.003$  MeV. The corresponding extraction uncertainties are estimated as 1 keV for  $B_{\Lambda}$  and 3 MHz for  $\Gamma$ . Recalling the high-momentum cutoff scale  $\Lambda_{\text{QCD}} \sim M_B$ , for a  ${}^3_{\Lambda}\text{H}$  averaged baryon mass  $M_B \approx 1$  GeV, we chose to work with  $\Lambda_{\text{UV}}=1$  GeV.

The main contributions to  $\Gamma_{\infty}^{\text{UV}}({}^3_{\Lambda}\text{H} \rightarrow {}^3\text{He} + \pi^-)$  at  $\Lambda_{\text{UV}}=1$  GeV, for both PW and DW pions, are listed in Table II. As seen, just three leading  ${}^3\text{He}$  and  ${}^3_{\Lambda}\text{H}$  configurations out of many other considered configurations reproduce within  $\lesssim 1\%$  uncertainty the total  ${}^3_{\Lambda}\text{H} \rightarrow {}^3\text{He} + \pi^-$

TABLE II: Partial decay rates  $\Gamma_{\infty}^{\text{UV}}(^3\Lambda\text{H}\rightarrow^3\text{He}+\pi^-)$  obtained by adding up fixed  $\Lambda_{\text{UV}}=1$  GeV contributions from three leading configurations in  $^3\text{He}$  and in  $^3\Lambda\text{H}$  are listed in GHz for PW and DW pions. Each of these  $l=0$  active-baryon ( $N, \Lambda, \Sigma$ ) configurations is specified by its spectator-nucleons isospin  $I$ , Pauli-spin  $S$ , orbital angular momentum  $L$  and total angular momentum  $J$ . Probabilities  $P$  are listed in percents. Total decay rates are given in the last row.

$(2I+1)(2S+1)L_J$	$P(^3\text{He})$	$P_{\Lambda}(^3\Lambda\text{H})$	$P_{\Sigma}(^3\Lambda\text{H})$	$\Gamma_{\text{PW}}^{\text{UV}}$	$\Gamma_{\text{DW}}^{\text{UV}}$
$^{13}S_1$	46.81	95.87	–	1.141	1.310
$+^{13}D_1$	48.42	99.23	–	1.219	1.398
$+^{31}S_0$	94.87	99.23	0.14	1.108	1.266
$L \leq 7 I, S \leq 1$	100	99.61	0.39	1.099	1.265

decay rate listed in the last row. Specifically, the dominant  $P(^3\Lambda\text{H})=96\%$  configuration in the first row corresponds to  $s_{\Lambda}$  hyperon coupled to a  $^3S_1$  quasi-deuteron that in  $^3\text{He}$  is close to the SU(4) limit of  $P=50\%$ . A few-percent  $^3D_1$   $NN$  component induced by the tensor force in both  $^3\text{He}$  and  $^3\Lambda\text{H}$  is added in the second row, almost saturating  $P(^3\Lambda\text{H})$ . About half of the remaining 0.8% probability arises from  $\Sigma NN$  configurations, induced by the  $\Lambda N \leftrightarrow \Sigma N$  transition component of the  $\chi\text{EFT } YN$  LO potential [17]. The leading such configuration, listed in the third row, is  $s_{\Sigma}$  hyperon coupled to a virtual-like  $^1S_0$   $NN$  component that in  $^3\text{He}$  is again close to the SU(4) limit of  $P=50\%$ . Remarkably, this tiny  $\Sigma NN$  admixture affects  $\Gamma_{\infty}^{\text{UV}}(^3\Lambda\text{H}\rightarrow^3\text{He}+\pi^-)$  more than the  $NN$  tensor force does, reducing the two-body decay rate by  $\approx 9\%$  as deduced by comparing the rates listed in the third row to those in the second row. The reduction is traced back to the sign of the  $\Lambda N \leftrightarrow \Sigma N$   $^1S_0$  contact term in the  $YN$  potential version used here; inverting this sign would reverse the sign of the observed charge symmetry breaking in the  $A=4$  hypernuclei [21]. The use of DW pions increases the PW two-body decay rate by  $\approx 15\%$ , inferred from the last row, higher than the  $\approx 10\%$  found in Ref. [12] where the pion optical potential was limited to its  $s$ -wave part; the larger DW effect found here owes to including its  $p$ -wave part. The two effects recorded here work in opposite directions, combining to a merely 3% increase of  $\Gamma_{\text{DW}}^{\Lambda+\Sigma}(^3\Lambda\text{H}\rightarrow^3\text{He}+\pi^-)$  with respect to  $\Gamma_{\text{PW}}^{\Lambda}(^3\Lambda\text{H}\rightarrow^3\text{He}+\pi^-)$  which is not listed here.

**From  $\Gamma(^3\Lambda\text{H}\rightarrow^3\text{He}+\pi^-)$  to  $\tau(^3\Lambda\text{H})$ .** To get the inclusive  $\pi^-$  decay rate  $\Gamma_{\pi^-}(^3\Lambda\text{H})$  from the two-body decay rate  $\Gamma(^3\Lambda\text{H}\rightarrow^3\text{He}+\pi^-)$  we use the branching-ratio value  $R_3 = \Gamma(^3\Lambda\text{H}\rightarrow^3\text{He}+\pi^-)/\Gamma_{\pi^-}(^3\Lambda\text{H})=0.35\pm 0.04$  [5]. Applying it to the two-body decay rate value 1.265 GHz associated in Fig. 1 with  $B_{\Lambda}(^3\Lambda\text{H})=159$  keV at  $\Lambda_{\text{UV}}=1$  GeV, and multiplying the obtained inclusive  $\Gamma_{\pi^-}(^3\Lambda\text{H})$  by the  $\Delta I = \frac{1}{2}$  factor  $\frac{3}{2}$  so as to include  $\Gamma_{\pi^0}(^3\Lambda\text{H})$ , the resulting pionic-decay  $^3\Lambda\text{H}$  lifetime is  $\tau_{\pi}(^3\Lambda\text{H})=184\pm 21$  ps, where the quoted uncertainty is statistical, arising from that of  $R_3$ . This calculated  $\tau_{\pi}(^3\Lambda\text{H})$  is shorter by  $(30\pm 8)\%$

than the free  $\Lambda$  lifetime  $\tau_{\Lambda}=263\pm 2$  ps. The total lifetime  $\tau(^3\Lambda\text{H})$  is shorter than that by (i)  $\approx 1.5\%$  from  $\Lambda N \rightarrow NN$  nonmesonic  $^3\Lambda\text{H}$  decay contributions [3, 36, 37]; and (ii)  $\approx 0.8\%$  from  $\pi NN \rightarrow NN$  pion true absorption in  $^3\Lambda\text{H}$  decay (mostly two-body) channels, estimated within our pion optical potential. The  $\approx 2.3\%$  summed yield of these non-pionic decay channels shortens slightly  $\tau_{\pi}(^3\Lambda\text{H})$ , leading to a  $^3\Lambda\text{H}$  lifetime  $\tau(^3\Lambda\text{H})=180\pm 21$  ps listed in the third row in Table III. It was tacitly assumed throughout this derivation of  $\tau(^3\Lambda\text{H})$  that the branching ratio  $R_3$  used here, taken from experiment [5], indeed corresponds to  $B_{\Lambda}(^3\Lambda\text{H})=159$  keV at which the input  $\Gamma(^3\Lambda\text{H}\rightarrow^3\text{He}+\pi^-)$  was evaluated.

TABLE III: Two-body decay rates  $\Gamma(^3\Lambda\text{H}\rightarrow^3\text{He}+\pi^-)$  (GHz) calculated for several  $\Lambda_{\text{UV}}$  cutoffs (MeV) from  $^3\Lambda\text{H}$  wavefunctions at given  $B_{\Lambda}$  values (keV), and as extrapolated to  $B_{\Lambda}=410$  keV, along with lifetimes  $\tau(^3\Lambda\text{H})$  (ps) evaluated using  $R_3=0.35\pm 0.04$  [5], the  $\Delta I = \frac{1}{2}$  rule, and an added 2.3% non-pionic decay rate.

$\Lambda_{\text{UV}}$	$B_{\Lambda}$	$\Gamma(^3\Lambda\text{H}\rightarrow^3\text{He}+\pi^-)$	$\tau(^3\Lambda\text{H})$
800	69	0.975	234 $\pm$ 27
900	135	1.197	190 $\pm$ 22
1000	159	1.265	180 $\pm$ 21
–	410	1.403	163 $\pm$ 18

**Relationship to  $B_{\Lambda}$ .** Expecting a lifetime  $\tau(^3\Lambda\text{H})$  close to  $\tau_{\Lambda}$  for a weakly bound  $\Lambda$  hyperon in  $^3\Lambda\text{H}$ , one might worry why the present fully microscopic UV-converged two-body rate calculation at  $\Lambda_{\text{UV}}=1$  GeV yielded, when augmented by a branching ratio  $R_3$  from experiment, a pionic lifetime  $\tau_{\pi}(^3\Lambda\text{H})$  shorter than  $\tau_{\Lambda}$  by as much as  $\sim 30\%$ . In response we draw attention to the considerably lower two-body rates marked in Fig. 1 for  $\Lambda_{\text{UV}}=800, 900$  MeV, where UV convergence has not yet been fully achieved. This means that some UV corrections that depend on short-range details of the employed interactions are missing in the extrapolation scheme of Eq. (6). Nevertheless, the correlation observed in the figure, for each value of  $\Lambda_{\text{UV}}$ , between  $\Gamma^{\text{UV}}(^3\Lambda\text{H}\rightarrow^3\text{He}+\pi^-)$  and its corresponding  $B_{\Lambda}^{\text{UV}}(^3\Lambda\text{H})$  appears robust. In particular the extrapolated two-body decay rates for  $\Lambda_{\text{UV}}=800, 900$  MeV provide meaningfully converged rates using well converged  $^3\Lambda\text{H}$  wavefunctions with  $B_{\Lambda}^{\text{UV}}=69, 135$  keV respectively. Repeating for these two-body decay rates the procedure that led to a relatively short lifetime value in the third row of Table III, using the same  $R_3$  value from experiment [5], we obtain for the least bound  $^3\Lambda\text{H}$  case a value shorter than  $\tau_{\Lambda}$  by only  $\sim 11\%$ , as listed in first row of Table III. This value of  $\tau(^3\Lambda\text{H})$  agrees reasonably with the most recent ALICE lifetime value and, within its  $R_3$  induced uncertainty, also with Kamada *et al.*'s lifetime value derived in a fully three-body calculation [38], both listed in Table I. Similarly, the lifetimes listed in the next two rows of Table III agree well within measure-

ment uncertainties with the HypHI lifetime value listed in Table I. Hence, as long as all  $B_\Lambda$  values within or close to the interval 0.07–0.16 MeV are acceptable, neither ALICE nor HypHI reported  ${}^3_\Lambda\text{H}$  lifetime values may be excluded. Given that the 50 keV uncertainty in the cited value  $B_\Lambda({}^3_\Lambda\text{H})=0.13\pm 0.05$  MeV [2] is purely statistical, and that a systematic uncertainty of the same size is plausible, a conservative estimate of the combined uncertainty is 0.07 MeV, so that all values of  $B_\Lambda({}^3_\Lambda\text{H})$  between 0.06 and 0.20 MeV are acceptable, and so are both ALICE’s and HypHI’s lifetime values.

To discuss more quantitatively STAR’s reported  $\tau({}^3_\Lambda\text{H})$  we extrapolate  $\Gamma({}^3_\Lambda\text{H}\rightarrow{}^3\text{He}+\pi^-)$  from the calculated values listed in the first three rows of Table III to a decay-rate value appropriate to  $B_\Lambda({}^3_\Lambda\text{H})=0.41$  MeV, the mean value claimed recently by the STAR Collaboration:  $B_\Lambda({}^3_\Lambda\text{H})=0.41\pm 0.12\pm 0.11$  MeV [13]. Expanding  $\Gamma({}^3_\Lambda\text{H}\rightarrow{}^3\text{He}+\pi^-)$  in powers of  $\sqrt{B_\Lambda}$ , with just linear and quadratic terms, we derive a value  $\Gamma({}^3_\Lambda\text{H}\rightarrow{}^3\text{He}+\pi^-)$  for  $B_\Lambda({}^3_\Lambda\text{H})=0.41$  MeV, as listed in the last row of the table. Repeating the procedure explained above of obtaining  $\tau({}^3_\Lambda\text{H})$ , we get  $163\pm 18$  ps which has substantial overlap with STAR’s reported lifetime [8] listed in Table I. In fact, had we used STAR’s listed own central value  $R_3=0.32$ , we would have obtained  $\tau({}^3_\Lambda\text{H})=149$  ps, almost coincident with STAR’s central lifetime value.

**Concluding remarks.** Reported in this work is a new microscopic three-body calculation of the  ${}^3_\Lambda\text{H}$  pionic two-body decay rate  $\Gamma({}^3_\Lambda\text{H}\rightarrow{}^3\text{He}+\pi^-)$ . Using the  $\Delta I = \frac{1}{2}$  rule and a branching ratio taken from experiment to connect to additional pionic decay rates, the lifetime  $\tau({}^3_\Lambda\text{H})$  was deduced. As emphasized here  $\tau({}^3_\Lambda\text{H})$  varies strongly with the small, rather poorly known  $\Lambda$  separation energy  $B_\Lambda({}^3_\Lambda\text{H})$ ; it proves possible then to correlate each one of the three distinct RHI experimentally reported values  $\tau_{\text{exp}}({}^3_\Lambda\text{H})$  with a theoretical value  $\tau_{\text{th}}({}^3_\Lambda\text{H})$  that corresponds to its own underlying  $B_\Lambda({}^3_\Lambda\text{H})$  value. The  $B_\Lambda({}^3_\Lambda\text{H})$  intervals thereby correlated with these experiments are roughly  $B_\Lambda \lesssim 0.1$  MeV,  $0.1 \lesssim B_\Lambda \lesssim 0.2$  MeV and  $B_\Lambda \gtrsim 0.2$  MeV for ALICE, HypHI and STAR, respectively. New experiments proposed at MAMI on Li target [39] and at JLab, J-PARC and ELPH on  ${}^3\text{He}$  target [40] will hopefully pin down precisely  $B_\Lambda({}^3_\Lambda\text{H})$  to better than perhaps 50 keV, thereby leading to a unique resolution of the ‘hypertriton lifetime puzzle’.

**Acknowledgments.** We are grateful to Patrick Achenbach, Nir Barnea, Peter Braun-Munzinger, Benjamin Dönigus, Alessandro Feliciello, Hans-Werner Hammer [41], Jiří Mareš and Satoshi Nakamura for useful remarks on a previous version. The work of DG was supported by the Czech Science Foundation, GAČR grant 19-19640S. Furthermore, the work of DG, EF and AG was partially funded by the European Union’s Horizon 2020 research & innovation programme, grant agreement 824093.

- 
- \* corresponding author, avragal@savion.huji.ac.il
- [1] A. Gal, E.V. Hungerford, and D.J. Millener, *Rev. Mod. Phys.* **88**, 035004 (2016).
  - [2] D.H. Davis, *Nucl. Phys. A* **754**, 3c (2005).
  - [3] M. Rayet and R.H. Dalitz, *N. Cimento* **46A**, 786 (1966).
  - [4] www.pdglive.lbl.gov, M. Tanabashi *et al.* (Particle Data Group), *Phys. Rev. D* **98**, 030001 (2018).
  - [5] G. Keyes, J. Sacton, J.H. Wickens, and M.M. Block, *Nucl. Phys. B* **67**, 269 (1973).
  - [6] C. Rappold *et al.* (HypHI Collaboration), *Nucl. Phys. A* **913**, 170 (2013).
  - [7] B.I. Abelev *et al.* (STAR Collaboration), *Science* **328**, 58 (2010).
  - [8] L. Adamczyk *et al.* (STAR Collaboration), *Phys. Rev. C* **97**, 054909 (2018).
  - [9] J. Adam *et al.* (ALICE Collaboration), *Phys. Lett. B* **754**, 360 (2016).
  - [10] S. Acharya *et al.* (ALICE Collaboration), *Phys. Lett. B* **797**, 134905 (2019).
  - [11] H. Kamada, J. Golak, K. Miyagawa, H. Witała, and W. Glöckle, *Phys. Rev. C* **57**, 1595 (1998).
  - [12] A. Gal and H. Garcilazo, *Phys. Lett. B* **791**, 48 (2019).
  - [13] J. Adam *et al.* (STAR Collaboration), *Nature Physics* **16**, 409 (2020).
  - [14] H. Le, J. Haidenbauer, U.-G. Meißner, and A. Nogga, *Phys. Lett. B* **801**, 135189 (2020).
  - [15] P.M.M. Maessen, T.A. Rijken, and J.J. de Swart, *Phys. Rev. C* **40**, 2226 (1989).
  - [16] A. Nogga, H. Kamada, and W. Glöckle, *Phys. Rev. Lett.* **88**, 172501 (2002).
  - [17] H. Polinder, J. Haidenbauer, and U.-G. Meißner, *Nucl. Phys. A* **779**, 244 (2006).
  - [18] J. Haidenbauer, U.-G. Meißner, A. Nogga, and H. Polinder, in *Topics in Strangeness Nuclear Physics*, Eds. P. Bydžovský, A. Gal, and J. Mareš, *Lecture Notes in Physics* **724**, 113-140 (2007).
  - [19] A. Nogga, *Nucl. Phys. A* **914**, 140 (2013).
  - [20] D. Gazda, J. Mareš, P. Navrátil, R. Roth, and R. Wirth, *Few-Body Syst.* **55**, 857 (2014).
  - [21] D. Gazda and A. Gal, *Phys. Rev. Lett.* **116**, 122501 (2016), and *Nucl. Phys. A* **954**, 161 (2016).
  - [22] M. Ablikim *et al.* (The BESIII Collaboration), *Nature Physics* **15**, 631 (2019).
  - [23] R.H. Dalitz and L. Liu, *Phys. Rev.* **116**, 1312 (1959).
  - [24] J.F. Donoghue, E. Golowich, and B.R. Holstein, *Dynamics of the Standard Model*, second edition (Cambridge University Press, Cambridge UK, 2014).
  - [25] E. Friedman and A. Gal, *Phys. Rep.* **452**, 89 (2007).
  - [26] E. Friedman and A. Gal, *Nucl. Phys. A* **928**, 128 (2014).
  - [27] E. Friedman and A. Gal, *Phys. Lett. B* **792**, 340 (2019).
  - [28] E. Friedman and A. Gal, *Acta Phys. Pol. B* **51**, 45 (2020).
  - [29] I. Schwanner, G. Backenstoss, W. Kowald, L. Tauscher, H.-J. Weyer, D. Gotta, and H. Ullrich, *Nucl. Phys. A* **412**, 253 (1984).
  - [30] R.A. Arndt, W.J. Briscoe, I.I. Strakovsky, and R.L. Workman, *Phys. Rev. C* **74**, 045205 (2006); see also SAID program <http://gwdac.phys.gwu.edu/>
  - [31] E. Friedman *et al.*, *Phys. Rev. Lett.* **93**, 122302 (2004), and *Phys. Rev. C* **72**, 034609 (2005).
  - [32] G. Backenstoss, J. Egger, T. von Egidy, R. Hagelberg, C.J. Herrlander, H. Koch, H.P. Povel, A. Schwitter, and

- L. Tauscher, Nucl. Phys. A **232**, 519 (1974).
- [33] B.D. Carlsson, A. Ekström, C. Forssén, D. Fahlin Strömberg, G.R. Jansen, O. Lilja, M. Lindby, B.A. Mattsson, and K.A. Wendt, Phys. Rev. X **6**, 011019 (2016).
- [34] R. Wirth, D. Gazda, P. Navrátil, and R. Roth, Phys. Rev. C **97**, 064315 (2018).
- [35] C. Forssén, B.D. Carlsson, H.T. Johansson, D. Sääf, A. Bansal, G. Hagen, and T. Papenbrock, Phys. Rev. C **97**, 034328 (2018).
- [36] J. Golak, K. Miyagawa, H. Kamada, H. Witała, W. Glöckle, A. Parreño, A. Ramos, and C. Bennhold, Phys. Rev. C **55**, 2196 (1997); Erratum: **56**, 2892 (1997).
- [37] A. Pérez-Obiol, D.R. Entem, and A. Nogga, J. Phys. Conf. Proc. Series **1024**, 012033 (2018).
- [38] Nogga *et al.* [16] observed that disregarding  $\Sigma NN$  components in  ${}^3_\Lambda\text{H}$  by limiting the  $YN$   $2\times 2$   $t$ -matrix to its diagonal  $\Lambda N$  element in a Faddeev calculation using the Nijmegen SC89  $YN$  interaction reduces the calculated  $B_\Lambda({}^3_\Lambda\text{H})$  from 143 keV to 27 keV. This might explain the relatively long  ${}^3_\Lambda\text{H}$  lifetime, close to  $\tau_\Lambda$ , reported in the  ${}^3_\Lambda\text{H}$  lifetime calculation by Kamada *et al.* [11].
- [39] P. Achenbach, S. Bleser, J. Pochodzalla, and M. Steinen, Proceedings of Science (**Hadron2017**), 207 (2018).
- [40] see talks at HYP2018: S.N. Nakamura, AIP Conf. Proc. **2130**, 020012 (2019), and A. Feliciello, *ibid.*, 020020.
- [41] Preliminary results on  $\tau({}^3_\Lambda\text{H})$ ,  $R_3$ , and their  $B_\Lambda$  dependence, derived in pionless EFT, were shown recently by Hans-Werner Hammer in a CERN Workshop, <https://indico.cern.ch/event/893621/timetable/>